Perceptual and Numerical Aspects of Spring Reverberation Modeling

Stefan Bilbao (1), Julian Parker (2)

(1) Acoustics and Fluid Dynamics Group/Music, University of Edinburgh, UK
(2) Department of Signal Processing and Acoustics, Aalto University, Helsinki, Finland

PACS: 43.40.Cw, 43.75.Tv, 43.75.Zz

ABSTRACT

The helical spring is a structure which has seen little investigation in the context of musical acoustics; though it does not play a role in musical instrument acoustics, it is the primary vibrating structure in electromechanical spring reverberation devices. The response of a spring is, however, even under linear conditions, far more complex than that of a straight rod, and consists of multiple echoes at distinct velocities, of a highly dispersive character, subject to multiple cutoff frequencies. In the interest of developing digital emulations, it is thus useful to obtain a complete picture of the perceptual importance of the various features in a reverberation context, through an investigation of dispersion curves and associated group velocities. Additional difficulties inherent in numerical simulation methods, also with an eye towrds perceptual considerations, will also be discussed.

INTRODUCTION

The vibration of a helical spring forms the basis for artificial spring reverberation [8, 20, 15], a popular classical electromehanical reverberation technique. Such units, while long since superseded by digital reverberation devices (normally based on sampled impulse responses or simple digital filter designs), possess certain special qualities which make emulation, through physical modeling methods, somewhat challenging. Such emulation of electromechanical and analog electronic audio effects has been quite popular recently—see, e.g., the recent special issue of the IEEE Transactions on Audio Speech and Language Processing [17] for a wide range of applications. Digital emulation of the spring reverberation unit has been approached using all-pass filter design techniques [1], delay lines [10] and finite difference schemes [4].

The typical response of a wire is complicated enormously, even under linear conditions, by the effects of curvature—the analysis of such behaviour is best approached in terms of dispersion curves, relating wavenumber to frequency, which exhibit regions in frequency of both low dispersion (leading to relatively coherent echoes) and high dispersion (leading to a more diffuse response or chirp-like echoes). Coherent echoes result purely from wire curvature, and are not present in a straight wire. More generally, such dispersion analysis allows for a means of extracting important perceptual attributes of the spring response, such as echo density, mode density and various cut-off frequencies—a necessary step in the calibration of an audio processing algorithm. Dispersion analysis has also been used, in the context of stiff string models, as a means of designing terminating filters for digital waveguide designs [3].

In this short paper, a model of helical spring dynamics will be presented, in the interest of determining features of perceptual interest—this is preliminary work, intended as an aid to future modeling work in conjunction with measured data, and especially to help in the analysis of spring responses, which are enormously complex. The model, suitable for thin springs, is a simple two-variable form reduced from a more complete thick-spring model and is detailed in the first section. In the next section, dispersion curves are derived, followed by an examination of the dependence of the curves on angle, cut-off frequencies, and the dependence of group velocity (and thus echo recurrence rates) on frequency and wavenumber. Some simple measured spring responses are examined subsequently in this light. Finally, there is a short discussion of the numerical issues in moving from a continuous problem to a discrete time framework (for digital emulation).

A THIN SPRING MODEL

The starting point in many investigations of helical spring dynamics is the model of Wittrick [18]—see, e.g., [19, 11]. Such a model, written as a system in twelve variables, incorporates effects of large thickness, and may be considered to be an extension of the Timoshenko theory of beam vibration [7] to the case of a beam with curvature. This system, which will not be presented here, possesses six dispersion relations, and captures the dynamics of the spring to very high frequencies (into the MHz range for springs of dimensions typical in reverberation applications). Given that (a) such springs are normally quite thin, (b) the range of frequencies of interest in audio applications is much lower (< 20 kHz), and normally only two of the six dispersion relations lie in the audio range and (c) computational expense will become an important issue if such a model is to be used, eventually, as a virtual emulation, a simpler "thin" spring model is a more useful starting point. (A comparison between the dispersion curves of the full model and the thin spring model appears later in this section.)

There are many such thin spring models, and it is important that the perceptual attributes of the model not be disturbed through such an approximation. One model, presented in [6], is similar to that given in [2] and other standard models of annular rings [7], and was used subsequently in [4] for virtual spring emulation. Such a model assumes zero helix angle (i.e., the spring is modelled as a series of rings), and faithfully approximates the lowest dispersion relation. However, as will be seen shortly, the dispersion characteristics of a spring de-

pend very strongly on angle—and furthermore, there are two closely spaced dispersion curves in the audio range. An angle-dependent two variable model, closely related to that given in [5] will be taken as the starting point here.

Model Equations

The geometry of a helical spring is as illustrated in Figure 1; indicated in the figure are the coordinate $x \in [0, L]$, representing arc length along the wire, of total unwound length L, as well as a transverse displacement v' (which is nearly parallel to the spring axis, when the helix angle is small), and a longitudinal displacement w' (which is in the direction of of the wire itself at any given point along the spring). In the model which follows, the displacements will be dependent on both the spatial coordinate x', and time t', i.e., $v' = v'(x', t')$, $w' = w'(x', t')$.
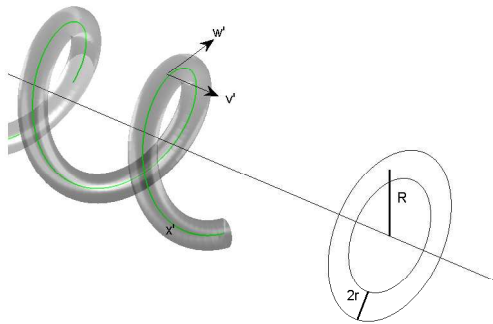

Figure 1: A helix, of wire radius r, and coil radius R. The coordinate x' (in green) runs along the midline of the wire, and displacements w' (longituidnal) and v' (transverse) are as indicated. .

The wire itself is of radius r, and of circular cross section, with cross sectional area $A = \pi r^2$ and moments of inertia I_v and I_w about the v and w directions. The coil radius is R, and the helix angle (in radians) is here written as α. (Angles in degrees will be written as $\angle$.) Material parameters for the spring are the density, ρ, in kg/m^3, and Young's modulus E and the shear modulus $G = \frac{1}{2}E/(1+\nu)$, for Poisson's ratio ν, both in Pa. In scaled coordinates, i.e., defining

$$x = x'\cos^2(\alpha)/R \quad v = v'\cos^2(\alpha)/R \quad w = w'\cos^2(\alpha)/R \quad (1)$$

and

$$t = t'/t_0 \qquad t_0 = \sqrt{\frac{\rho A R^4}{E I_v \cos^4(\alpha)}} \qquad (2)$$

the following simplified model of spring dynamics follows directly from the general model of Wittrick, under the assumption that the spring is thin:

$$\mathbf{A}\mathbf{u}_{tt} = \mathbf{Q}\mathbf{m}_x \quad \mathbf{D}\mathbf{m} = \mathbf{Q}\mathbf{u}_x \qquad (3)$$

Here, $\mathbf{u} = [v, w]^T$ is a vector containing the transverse and longitudinal displacements, and subscripts t and x indicate partial differentiation with respect to x and t. The matrix operators $\mathbf{A}$, $\mathbf{D}$ are defined as

$$\mathbf{A} = \begin{bmatrix} 1 & 0 \\ 0 & 1 - \frac{\partial^2}{\partial x^2} \end{bmatrix} \quad \mathbf{D} = \begin{bmatrix} 1 & 0 \\ 0 & d - \frac{\partial^2}{\partial x^2} \end{bmatrix} \qquad (4)$$

and the operator $\mathbf{Q}$ as

$$\mathbf{Q} = \begin{bmatrix} -2\tau & \tau^2 - 1 - \frac{\partial^2}{\partial x^2} \\ \tau^2 - 1 - \frac{\partial^2}{\partial x^2} & 2\tau \left(1 - \frac{\partial^2}{\partial x^2}\right) \end{bmatrix} \qquad (5)$$

In this non-dimensional form, the system depends on the two parameters

$$\tau = \tan(\alpha) \quad d = E I_w / G I_v \qquad (6)$$

Such a two-variable model is very similar to that given in [5] (the discrepancy may be due to an error in this article, in Equation 5). These same authors give a value of $d = 1.3$, for a spring of circular cross-section, and for Poisson's ratio 0.3.

Not presented here are the boundary conditions, six of which must be supplied at each end of the spring.

DISPERSION CURVES AND EIGENSTRUCTURE

Dispersion curves for system (3) follow directly, under the assumption of a wave-like solution, of angular frequency ω and wavenumber β. The system may then be written, at steady state, as

$$\omega^2 \hat{\mathbf{u}} = \mathbf{R}\hat{\mathbf{u}} \qquad \mathbf{R} = \beta^2 \hat{\mathbf{A}}^{-1} \hat{\mathbf{Q}} \hat{\mathbf{D}}^{-1} \hat{\mathbf{Q}} \qquad (7)$$

where $\hat{\mathbf{u}}$ is a vector of complex amplitudes, and where the matrices above become, in terms of wavenumber β,

$$\hat{\mathbf{A}} = \begin{bmatrix} 1 & 0 \\ 0 & 1 + \beta^2 \end{bmatrix} \quad \hat{\mathbf{D}} = \begin{bmatrix} 1 & 0 \\ 0 & d + \beta^2 \end{bmatrix} \qquad (8)$$

$$\hat{\mathbf{Q}} = \begin{bmatrix} -2\tau & \tau^2 - 1 + \beta^2 \\ \tau^2 - 1 + \beta^2 & 2\tau \left(1 - \beta^2\right) \end{bmatrix} \qquad (9)$$

Dispersion curves may be derived easily by taking the eigenvalues of $\mathbf{R}(\beta)$; if $\lambda^+(\beta)$ and $\lambda^-(\beta)$ are the two eigenvalues (both positive), then the dispersion relations $\omega^+(\beta)$ and $\omega^-(\beta)$ are given simply as

$$\omega^+(\beta) = \sqrt{\lambda^+(\beta)} \qquad \omega^-(\beta) = \sqrt{\lambda^-(\beta)} \qquad (10)$$

For reference, in Figure 2 at top, the two curves are plotted, as a function of β, for a spring of thickness typical of spring reverberation units, and for a helix angle of $\angle = 5°$. The difference between the curves generated by system (3) and the full twelve variable model is shown at bottom; it is most pronounced at high wavenumbers, and is negligible over most of the audio range.
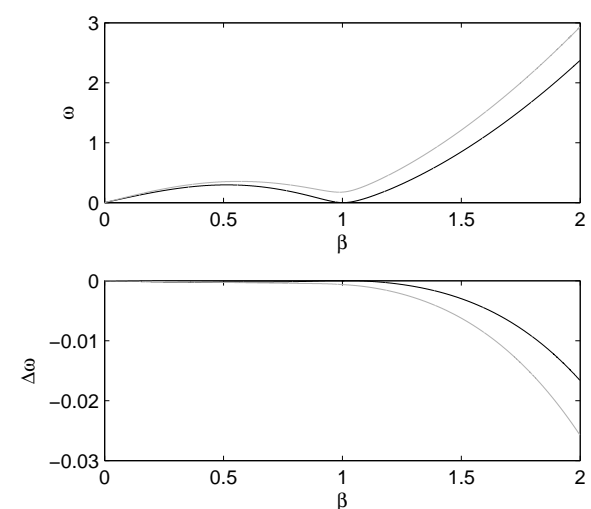

Figure 2: Top: non-dimensional dispersion curves $\omega^+(\beta)$ (grey) and $\omega^-(\beta)$ (black) for the model (3). Bottom: Difference $\Delta\omega$ between curves generated by model (3), and a full twelve-variable model, incorporating effects of thickness. In this case, the spring has $\tau = 0.0875$, and $d = 1.3$.

General Features

The two curves possess a similar form. Each exhibits a primary hump covering the range of wavenumbers between $\beta = 0$ and $\beta \cong 1$, and reaching a peak at a wavenumber slightly above $\beta = 0.5$; the hump is thus not symmetric, even in the limit of small angle. The lower (-) curve possesses a zero at $\beta = 0$, and an additional zero at $\beta = \beta_0 = \sqrt{1 + \tau^2}$. At $\beta = \beta_0$, the motion of the spring is thus rigid body, where the corresponding wavelength is exactly one turn of the helix. At wavenumbers above the primary hump, both curves approach bar-like dispersion curves, with a general dependence on β^2.

Dependence on Angle

The general shapes of the curves exhibit large variation, even for very small angles (which are normally on the order of between 1 and 4 degrees for spring reverberation units). See Figure 3. The lower curve retains a zero at $\beta = \beta_0 = \sqrt{1 + \tau^2}$, but becomes progressively smoother as angle increases. The upper curve, however, possesses a minimum which increases with angle, until an angle of approximately $\angle = 14°$, after which it becomes purely monotonic. Notive that the curves are not identical when the helix angle is zero; at zero helix angle, the system decouples into pure longitudinal and transverse motion.
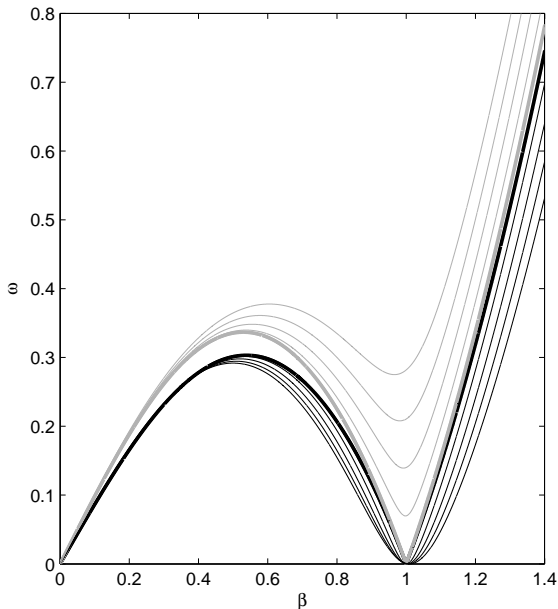

Figure 3: Variation of dispersion curves $\omega^+(\beta)$ (grey) and $\omega^-(\beta)$ (black) with helix angle for the model (3). The thick curves represent the uncoupled dispersion relations when $\angle = 0°$, and moving progressively away from them are curves with $\angle = 2°, 4°, 6°, 8°$

Cut-off Frequencies

There are various cutoff frequencies associated with the system, allowing the determination of the number of wavelike and evanescent solutions in a given frequency range. The lower curve ω^+ possesses a maximum at (for very low angles),

$$\omega_{c+}^{(-)} \cong 0.3 \qquad \text{at} \qquad \beta \cong 0.53$$

and similarly, for the upper curve,

$$\omega_{c+}^{(+)} \cong 0.34 \qquad \text{at} \qquad \beta \cong 0.53$$

These are indicated as horizontal black and grey dotted lines, respectively, in Figure 4.

In spring reverberation units, these cutoffs (in dimensional units) normally occur in the range between 2 and 5 kHz, and constitute one of the major perceptual features of a spring reverberation unit, the sound of which is primarily low-passed, with a superimposed high-frequency noise-like component.
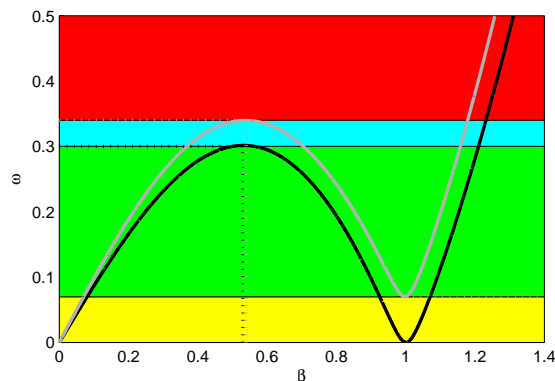

Figure 4: Dispersion curves for system (3), where the helix angle is $\angle = 4°$. Cutoff frequencies are indicated by horizontal dotted lines, and regions over which there are distinct numbers of traveling components to the solution by different colors.

In addition to the high-frequency cutoffs, the (+) curve possesses an additional low-frequency cutoff slightly below $\beta = 1$. For low angles, the cutoff occurs at approximately

$$\omega_{c-}^{(+)} = 2\tau \qquad\qquad (11)$$

which is indicated as a horizontal dotted grey line in Figure 4. This frequency is normally under 1 kHz for a typical spring reverberation unit.

Traveling and Evanescent Components

The number of intercepts of the pair of curves at a given frequency indicates the number of traveling (i.e., real wavenumber) components to the solution at this frequency. Regions of distinct numbers of traveling components are indicated by colors in Figure 4. Below $\omega_{c-}^{(+)}$, thus, there are four such solutions (in yellow); between $\omega_{c-}^{(+)}$ and $\omega_{c+}^{(-)}$ there are six (in green); between $\omega_{c+}^{(-)}$ and $\omega_{c+}^{(+)}$ there are four (in blue); and above $\omega_{c+}^{(+)}$ (at least until the range of very high frequencies, at which point the full thick spring model will be necessary for a complete count), two (in red). Such waves are uni-directional—for the spring system, there will be a symmetric set of components traveling in the opposite direction, thus the total number of traveling components will be twice the count here.

This characterization is valid, provided that boundary conditions are not frequency dependent—but is a spring reverberation unit, they may well be slightly so, due to the nature of the excitation mechanism (essentially a massive bead fixed to one end of the spring and driven electromagnetically), and the pickup (a similar bead moving within a magnetic field at the opposite end).

Group Velocity and Echoes

One of the interesting features of spring reverberation units is the strong presence of coherent echoes in the resulting response; as mentioned above, such echoes are notably absent in other electromechanical reverberation devices (such as plate reverberation [9]), and are more prominent than in the case of a straight wire.
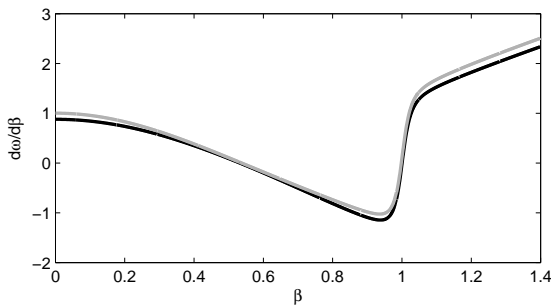
Figure 5: Group velocity curves $d\omega^+/d\beta$ (grey) and $d\omega^-/d\beta$ (black) for the model (3), with helix angle $\angle = 2°$.

To this end, it is interesting to examine the behaviour of the group velocity curves associated with the dispersion curves $\omega^{(+)}$ and $\omega^{(-)}$, which may be obtained by differentiation with respect to wavenumber β. The two curves are shown in Figure 5. Regions over which the curves are relatively flat correspond to coherent wave propagation; of particular interest are the limiting values of the curves in the limit as β approaches zero:

$$v_g^{(+)} \cong 1 \qquad v_g^{(-)} \cong 1/\sqrt{d} \le 1 \qquad (12)$$

Complicating the analysis of measured responses somewhat, in the low frequency ranges, is the presence of not merely the coherent echo set near $\beta = 0$, but the also somewhat less coherent set which may be observed from the flat portion of the group velocity curves near $\beta = 1$—which, from the dispersion relation, lie in the same frequency range as the set mentioned above. There are thus four distinct wave speeds very close to 1 in the range of low frequencies.

Echo densities may be estimated (roughly) by dividing the group velocity by the unwound spring length. Spring reverberation units are often designed such that this density is between 20/s and 50/s.

MEASURED SPRING RESPONSES

In a preliminary study, spring response measurements were taken from a Belton MB3BB2C1B spring reverberation unit driven by a Doepfer A-199 spring driver/preamp unit. Responses were obtained using a sine-sweep method with a sweep-time of 10 seconds. Individual springs (of the three in the unit) were measured by damping the other springs using foam. The spring responses shown in this section are all drawn from a single spring, made of stainless steel, and of helix angle $\angle = 2.2°$.

A spectrogram of a spring response is shown in Figure 6. Though the response is rather complex, various features are readily apparent. First, there is a clear cutoff in the region of approximately 3 kHz, and, below it, a main series of echoes (which appears as a set of black arcs in the spectrogram) which lags progressively towards this cutoff, thus illustrating the slowdown in velocity in the region of the primary cutoffs (see Figure 5). In the region of the first reflections, clear secondary echoes are also visible, with an echo density slightly different from that of the main series. Above the cutoff, the response is much simpler, and consists of a series of echoes, for which velocities increase with frequency—this is the region of a pure bar-like response, corresponding to the rightmost branches of the dispersion curves as shown in Figure 2.

There are various features which are not adequately explained by the model—one is the presence of a transition at approximately 5 kHz, which could well be due to a resonance of the driving mechanism (essentially a mass-spring system).
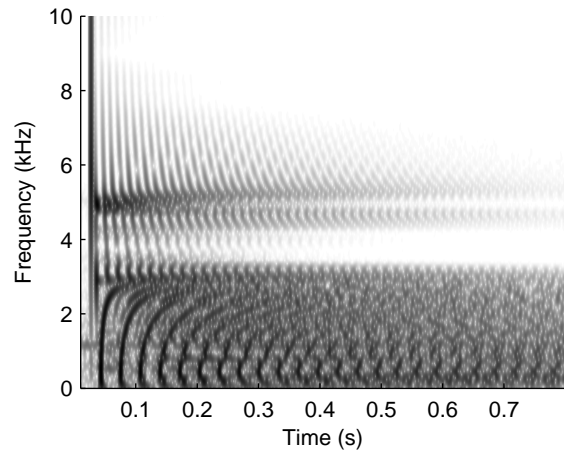

Figure 6: Spectrogram of a spring impulse response.

Most interesting are discrete transition frequencies, below the primary cutoff, dividing series of echoes which propagate at close but distinct velocities; these are visible in Figure 7, showing three such transitions in the 0 to 1.5 kHz range. It is fairly clear that these must correspond to regions of distinct group velocity over the available branches of the dispersion curves shown in Figure 2 (as many as six). The nature of these discrete transitions (as opposed to a continuous mixing of waves of all possible speeds at a given frequency) is not clear. The crossover is also easily visible in a spectral plot of the impulse response, as shown in Figure 8; the transition may be seen as a region of superposition of two families of nearly equally spaced components.

Yet another interesting feature is that, above the primary cutoff, instead of a double series of echoes, corresponding to both branches of the dispersion curves in this region, a clear single set is visible; a full analysis of boundary conditions is necessary to determine which of the two types of motion is dominant over such a frequency range.
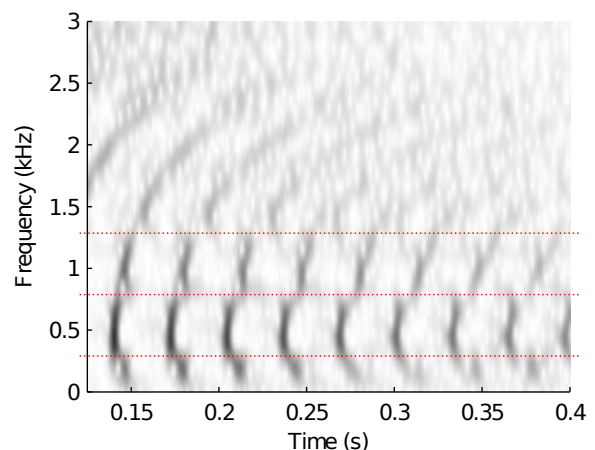

Figure 7: Detail of a spectrogram of a spring impulse response, illustrating transitions between families of echoes with distinct velocities over different frequency regions; transition frequencies are indicated by red lines.

NUMERICAL CONSIDERATIONS

The simulation of spring vibration, even using a simplified model such as that presented here, presents great challenges
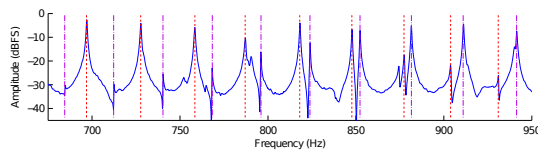
Figure 8: Detail of spectrum of the spring impulse response, showing a transition between two distinct families of relatively equally spaced peaks.

numerically—ideally, one would like an algorithm which takes, as input parameters, the sample rate and the various geometric and material constants which define the spring (or, perhaps, the reduced parameter set consisting of d, τ and t_0), apply an input signal, and obtain a reverberant output. It is also obviously preferable to have an algorithm which operates at a reasonably low sample rate, and with minimal computational and memory requirements both in the main run time loop operating at the sample rate, and in terms of precomputation before run time. The various techniques which are used in physical modeling applications all lead to various distinct difficulties in the present case of the spring; here, the hurdles to be overcome (which are not insurmountable!) will be outlined in brief.

Digital Waveguides

Digital waveguides [14] have been used with great success in the simulation of 1D linear systems exhibiting low dispersion, such as, e.g., strings, and acoustic tubes of nearly cylindrical or conical bore brofile; indeed, as the structure consists of a delay line, with effects of dispersion and loss lumped in low-order terminating filters, they can be far more efficient than virtually any other simulation technique.

The low dispersion mentioned above, in, e.g., strings, leads to a monotonically increasing dispersion relation, or, in other words, a wave velocity of a traveling component which increases with frequency, leading to perceived inharmonicity. In the waveguide context, a practical solution is the insertion of all-pass filter structures at the termination of the waveguide, leading to the desired variable group velocity. Even in this simple example, there are two points worth mentioning:

First, in a stiff string, evanescent components will be present, and there is as yet no known mechanism for representing such components in a delay line structure. Linked to this phenomenon is the need for specifying an additional boundary condition at either end of the string; such additional conditions have also not been addressed in the literature. In strings, effects of stiffness are normally quite small, so this is not a matter of concern in audio simulation, but for stiffer structures such as bars, the precise form of the boundary conditions leads to great differences in perceived sound output.

Second, the order of the terminating correction filter is small when dispersion is low, but can become quite large under higher stiffness; thus, the efficiency advantage of a waveguide formulation is progressively lost as stiffness increases.

Now consider the present case of the helical spring; at any given frequency, there are as many as six distinct wave velocities. This implies a structure which would require six digital waveguides, or bidirectional delay line pairs, each with an associated termination filter allowing for variation in group velocity with frequency. There are several open questions: As before, there is the issue of the representation of evanescent components, which in contrast to the case of the string, are present in a number which depends on frequency; linked to this is again the need for setting boundary conditions, leading to a coupled

termination among the waveguides. A more delicate issue is that of the non-monotonicity of the dispersion curves—zero group velocity is attained at a non-zero wavenumber, implying an infinite-length (or, in practice, extremely long) delay line.

Modal Methods

The helical spring, given that its behaviour is presumably linear (at least in audio applications), and that input and output are applied and read at locations which are not varied, is a good candidate for a modal approach. Given system (3), and a set of six boundary conditions at either end of the spring, one may, in theory, solve for the modal frequencies and shapes (or, in this case, the amplitudes of the modal functions at the input and output locations), and an exceedingly simple structure results, relying on uncoupled digital oscillators ("two-poles"). An additional bonus is complete control over damping for individual components, which may be set directly from measured responses. Modal methods have been used extensively in physical modeling of musical instruments [13].

The most straightforward means of obtaining modal data is through a steady-state approximation to (3) through, e.g., finite element, or finite difference methods; the spatial derivatives are discretized over a grid, with boundary conditions taken into account, and an eigenvalue problem results. This is a common approach in mechanical engineering applications, but must be used with caution in an audio setting for the following reasons: (a) in most industrial applications, one is interested mainly in a few low frequency modes; such is not the case in audio, where one requires good accuracy over the entire spectrum (consisting of between 400 and 1000 modes for a typical spring reverberation unit) and (b) one may need to make use of a very large number of degrees of freedom (far greater than the number of modes) in order to obtain good accuracy—such computation must be performed off-line, and can thus introduce noticeable latency in an audio application.

As an alternative, instead of solving the eigenvalue problem directly, employ the dispersion curves directly, and solve for $\beta(\omega)$, yielding twelve solutions. The twelve required boundary conditions (six at either end of the spring) may then be used to construct a 12×12 matrix $\mathbf{B}(\omega)$, whose determinant will vanish at a modal frequency of the system. In order to determine the modal frequencies of the system, one may then step through the determinant with ω, and search for changes in sign of this determinant. Such a procedure is functionally similar to the dynamic stiffness method employed by some authors [11], and has the advantage of allowing the determination of the modal frequencies to arbitrary accuracy. Here too, there are numerical difficulties—modal frequencies can be extremely close together, and one may need to step through the determinant using a very small increment in frequency, and above the primary cutoff, where evanescent solutions are present, numerical scaling issues can become very severe.

Finite Difference Time Domain Methods

In theory, a finite difference approximation to the helical spring system should be able to sidestep all the difficulties mentioned above; there is also no heavy precomputation of the type associated with modal methods.

The problem, in the case of FDTD is numerical dispersion—a direct discretization of system (3) using second-order difference schemes yields very poor results—see Figure 9, illustrating dispersion relations for the model system, and numerical dispersion relations for a simple FD scheme. At a reasonable audio sample rate (in this case, non-dimensional, but corresponding to 44.1 kHz), the scheme is only correct at very low

frequencies, and is unable to capture many important features, such as cutoffs; in particular, the high-frequency wave speeds above the cutoff will be wildly inaccurate.
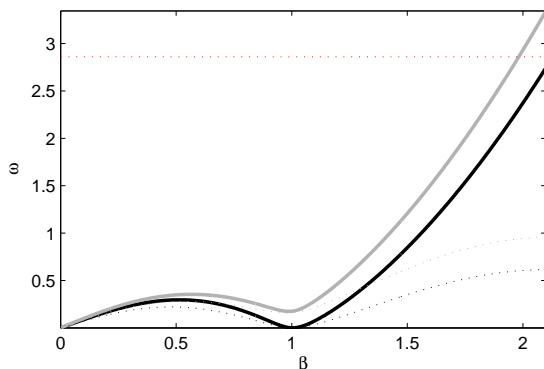

Figure 9: Dispersion relations for the model system (solid lines) and for a simple FD approximation (dotted lines). The sampling frequency (non-dimensional) is shown as a red dotted line.

There are two remedies. One is to work at a much higher audio rate (generally, at least 200 kHz will be required for a perceptually accurate simulation), which can be prohibitively expensive, given that system (3) will require, by its very nature, an implicit numerical method. Another is to make use of a more accurate scheme, and there are many choices. Higher-order accurate time stepping schemes, in conjunction with accurate approximations to spatial derivatives are one possibility, and do a much better job of approximating the system over the low frequency range, but are still unable to capture the behaviour of the system above the primary cutoff—the same is true of, e.g., pseudospectral methods [16], which will giving very high accuracy at low frequencies, generally exhibit a very high degree of dispersion at higher frequencies and artificial bandlimiting. A better choice is a parameterized low-order scheme (compact implicit [12]), optimized to match the dispersion relation of the model system over a given frequency range, and which operates at a reasonable audio sample rate. Such schemes are presently under study. Needless to say, a good finite difference approximation can also be used as a means of obtaining modal data.

CONCLUDING REMARKS

This paper is intended as a rough sketch of the dynamics of spring reverberation units, and to indicate some of the perceptual features of interest; the model presented here is simplified as far as possible from a more complete model, and it is doubtful that further simplification is possible without losing perceptually salient features of the spring. Even still, as has been noted above, there are features of measured responses which are as yet not well explained by this model. Numerically, the problem of simulation of helical spring dynamics is a very delicate one, regardless of the method one employs; the difficulties are distinct, however, depending on the type of method employed.

The model presented here is lacking is several features. One is a model of loss; though generally small for reverberation devices, it is clearly frequency-dependent to a high degree, as is clearly evident in Figure 6; loss will result from effects of radiation in the spring itself (presumably quite small), internal losses in the spring (larger), and due to the (as yet unmodelled) driving mechanism, which has a built-in damping mechanism. Another, very important consideration which has not

been discussed here, is the precise set of boundary conditions to be applied (six) at either end of the spring—this must also include the coupling to the excitation and readout mechanisms. Though conditions in the longitudinal direction are fairly easy to deduce, the conditions on transverse motion are harder to ascertain, and there are numerous choices.

The measurements described here are not intended for serious study, but for a first look at some of the properties of the response of a spring reverberation unit. They have been taken directly from the pickup, and thus the effects of the driving mechanism, as well as the accompanying electronics are all present. In a more rigorous study, one would of course want to make pure acoustical measurements of the spring behaviour in the absence of electronic amplification; such work is under way.

REFERENCES

[1] J. Abel, D. Berners, S. Costello, and J. O. Smith III. Spring reverb emulation using dispersive allpass filters in a waveguide structure. Presented at the 121st Audio Engineering Society Convention, San Francisco, California, October, 2006. Preprint 6954.

[2] C. Riedel B. Kang and C. Tan. Free vibration analysis of planar curved beams by wave propagation. *Journal of Sound and Vibration*, 260:19–44, 2003.

[3] J. Bensa, S. Bilbao, R. Kronland-Martinet, and J. O. Smith III. The simulation of piano string vibration: From physical models to finite difference schemes and digital waveguides. *Journal of the Acoustical Society of America*, 114(2):1095–1107, 2003.

[4] S. Bilbao and J. Parker. A virtual model of spring reverberation. *IEEE Transactions on Audio Speech and Language Processing*, 14(2):695–705, 2010.

[5] L. Della Pietra and S. della Valle. On the dynamic behaviour of axially excited helical springs. *Meccanica*, 17:31–43, 1982.

[6] N. Fletcher, T. Tarnopolskaya, and F. de Hoog. Wave propagation on helices and hyperhelices: A fractal regression. *Proceedings of the Royal Society*, 457:33–43, 2001.

[7] K. Graff. *Wave Motion in Elastic Solids*. Dover, New York, New York, 1975.

[8] L. Hammond. Electical musical instrument, February 2 1941. US Patent 2,230,836.

[9] W. Kuhl. The acoustical and technological properties of the reverberation plate. *E. B. U. Review*, A(49), 1958.

[10] R. Kuroki. Sound effect imparting apparatus , January 26 1999. US Patent 6,580,796.

[11] J. Lee and D. Thompson. Dynamic stiffness formulation, free vibration and wave motion of helical springs. *Journal of Sound and Vibration*, 239(2):297–320, 2001.

[12] S. Lele. Compact finite difference schemes with spectral-like resolution. *Journal of Computational Physics*, 103:16–42, 1992.

[13] D. Morrison and J.-M. Adrien. Mosaic: A framework for modal synthesis. *Computer Music Journal*, 17(1):45–56, 1993.

[14] J. O. Smith III. *Physical Audio Signal Procesing*. Stanford, CA, 2004. Draft version. Available online at http://ccrma.stanford.edu/~jos/pasp04/.

[15] J.D. Stack. Sound reverberating device, March 9 1948. US Patent 2,437,445.

[16] L. Trefethen. *Spectral Methods in Matlab*. SIAM, Philadelphia, Pennsylvania, USA, 2000.

[17] V. Välimäki, U. Zölzer, and J. O. Smith, editors. 2010. IEEE Transactions on Audio Speech and Language Processing: Special Issue on Virtual Audio Effects and Musical Instruments.

[18] W. Wittrick. On elastic wave propagation in helical springs. *International Journal of Mechanical Sciences*, 8:25–47, 1966.

[19] V. Yildrim. Investigation of parameters affecting free vibration frequancy of helical springs. *International Jounral for Numerical Methods in Engineering*, 39:99–114, 1996.

[20] A.C. Young and P. It. Artificial reverberation unit, October 8 1963. US Patent 3,106,610.